JOURNAL OF AIRCRAFT
Vol. 56, No. 2, March–April 2019

Optimal Airspeeds for Scheduled Electric Aircraft Operations

Thomas Hamilton* and Brian J. German†
Georgia Institute of Technology, Atlanta, Georgia 30332

DOI: 10.2514/1.C035051

The potential for reductions in emissions, energy costs, and maintenance costs has led to interest in battery-electric propulsion for small aircraft. However, the low specific energy of current batteries considerably limits aircraft range, payload, and speed performance. Additionally, recharge power limitations impede the ability to recharge quickly between flights, restricting the feasibility of electric aircraft for scheduled operations. This paper considers the problem of choosing the cruise airspeeds of different flights within a schedule to maximize the energy feasibility of the schedule, subject to the constraints of a fixed timeline of departures. Two types of schedules are considered: one in which every route is the same and repeating, and one in which every route may be unique. This optimization problem results in airspeeds that balance energy expended during cruise and energy replenished during recharge. A greedy algorithm is presented to determine these optimal airspeeds for schedules with unique routes.

Nomenclature

b	=	wingspan
C_{D0}	=	coefficient of zero-lift drag
D	=	drag
D_B	=	minimum drag in steady, level flight
D_I	=	induced drag
D_0	=	zero-lift drag
e	=	Oswald efficiency
F	=	finite repeating route-schedule factor
i	=	route index
L	=	lift
n	=	total number of flights in the schedule
P	=	recharge power
P_B	=	minimum power consumption in steady, level flight
R	=	distance of flight
S	=	wing area
V	=	airspeed
V_B	=	airspeed for minimum drag in steady, level flight
V_E	=	airspeed for equal discharge and recharge energy
V_G	=	greedy policy airspeed
V_S	=	minimum airspeed allowed by schedule
V_χ	=	airspeed for maximum final charge of a route
V'_χ	=	airspeed for maximum final charge of n repeated routes
W	=	gross weight
W_b	=	battery weight
W_p	=	payload weight
Δt	=	time available for flight and recharge
Δt_r	=	recharging time period
$\Delta\chi_f$	=	charge lost due to a flight
$\Delta\chi_n$	=	net charge lost after flight and recharge
$\Delta\chi_r$	=	charge recovered due to recharging
ϵ	=	effective battery energy per weight
η_p	=	propulsive efficiency
ρ	=	density of atmosphere
χ	=	state of charge
χ_a	=	state of charge on arrival
χ_d	=	state of charge before departure
$\chi_{\text{ms},i}$	=	minimum state of charge of routes $i+1$ through n
χ_T	=	minimum state-of-charge feasibility threshold

Presented as Paper 2017-3284 at the 17th AIAA Aviation Technology, Integration, and Operations Conference, Denver, CO, 5–9 June 2017; received 8 April 2018; revision received 9 August 2018; accepted for publication 14 August 2018; published online 7 December 2018.

*Graduate Research Assistant, School of Aerospace Engineering, 270 Ferst Drive. Student Member AIAA.

†Langley Associate Professor, School of Aerospace Engineering, 270 Ferst Drive. Associate Fellow AIAA.

I. Introduction

As BATTERY technologies mature, aircraft electric propulsion is becoming increasingly promising because of the potential to reduce operating costs and improve environmental sustainability. Electricity can be procured less expensively and with less environmental impact than hydrocarbon fuels in many energy markets. Preliminary evidence suggests that electric propulsion systems may also be less expensive to maintain than fuel-burning aircraft engines [1]. However, at present, the specific energy of a battery-electric propulsion system is much lower than an equivalent hydrocarbon system, making it more difficult to obtain an aircraft design with a practical range, payload, and speed. Even so, the range capability of electric aircraft may be suitable for emerging short-range markets, including urban air mobility (UAM) and thin-haul aviation [2]. The economics of these markets is promising [3], particularly if the anticipated energy and maintenance cost advantages of electric aircraft relative to traditional aircraft can be realized [2,4].

Scheduled operations present an additional challenge for battery-electric aircraft, because the aircraft must be recharged quickly within limited ground time intervals to maintain a productive flight schedule. For a traditional fuel-burning aircraft, a flight's worth of fuel can be pumped in a few minutes, well within the time frame of normal ground operations. A comparable electric aircraft, however, may require an hour or more to recharge the energy required for a flight, as determined by the allowable recharge power. Recharge power can be limited based on considerations of battery chemistry and cooling, recharger equipment, or electricity demand costs.

If an electric aircraft were forced to maintain a sufficiently fast-paced schedule without an adequate recharge time, net battery discharge would build up during the day. The aircraft would repetitively expend more energy on each flight than it recoups by recharging. The implication of such a situation is that either the aircraft must be oversized with a larger battery to overcome the net energy shortfall, or the departure schedule must be relaxed to allow an increased time for recharging.

In this context, one may hypothesize that a viable strategy may be to fly certain routes at faster speeds than the classical maximum range airspeed to enable more recharging time on the ground between flights. As shown in Sec. IV.B, under certain circumstances, such a strategy will indeed yield an increased battery state of charge at the beginning of the subsequent flight. Increased charging time potentially enables the vehicle to fly more routes, longer routes, or otherwise more challenging schedules, thus increasing the overall feasibility of operations.

This paper considers this problem of choosing the airspeeds of a battery-electric aircraft to maximize the energy feasibility of flight schedules. The paper is organized as follows. Section II provides context and background information relevant to this problem. A schedule model, vehicle model, flight profile, and airspeed optimization problem are formulated in Sec. III. This formulation is used in Sec. IV to derive airspeeds that are generally important to the route-schedule problem. A key contribution of this paper, provided in Sec. IV.B, is the identification of the airspeed that trades flight energy for airspeed to maximize the energy available for subsequent flights. Two types of schedules are then considered: Sec. V considers schedules in which every route is the same and repeating, and Sec. VI considers schedules in which every route is unique. Section VII provides numerical example results for these two schedule types. Finally, Sec. VIII describes a way to extend the aforementioned analyses to more general mission profiles.

II. Background in Electric Aircraft Range Estimation and Optimization

Several Breguet-like range equations for battery-electric aircraft have been developed in prior work in the literature. The simplest models typically neglect the details of battery discharge performance, and instead model the battery in terms of a constant value of specific energy. For example, a range equation for battery-electric propeller-driven aircraft with constant battery specific energy can be expressed as [5,6]

$$R = \frac{L}{D} \cdot \frac{W_b}{W} \cdot \eta_p \cdot \epsilon \cdot \chi \tag{1}$$

Here, ϵ is the pack-level battery specific energy (i.e., the effective battery energy per battery weight). In this simple formulation, ϵ must be interpreted to account for any weight penalty associated with the integration of cells into the battery pack, and any capacity and voltage degradation associated with discharge current, battery aging, and operating conditions. In general, ϵ varies with operating conditions and, in particular, with the discharge current profile. When adopting an approximate constant value for ϵ, accuracy is improved when the operating voltage and current are close to the voltage and current at which the parameter is measured. The parameter χ is the initial state of charge of the battery. Equation (1) has been used for aircraft performance, sizing, and performance studies [5,6], and is fundamental to the analysis presented in this paper.

More sophisticated range equations have been developed based on more advanced battery discharge models. For example, Traub developed a range equation that leverages Peukert's law [7]. Peukert's law accounts for variation of capacity with discharge current, which results in lower net energy delivered to the load as current is increased [8]. Traub also derived and validated optimal endurance and range conditions for battery-electric aircraft [7,9]. Another example can be found in the work of Avanzini and Giulietti, who developed similar models to account for battery-capacity variation with discharge conditions [10]. An empirical battery model developed by Avanzini et al. was used to derive closed-form performance equations for optimal range and endurance, as was done with the Peukert model [11]. Both Avanzini et al.'s and Traub's equations have also been used for aircraft sizing [11,12].

Falck et al. demonstrated an approach for trajectory optimization for electric aircraft to maximize the range performance [13]. They incorporated thermal effects in the battery model and in models of other electric propulsion components. Their approach determined optimal flight profiles, in terms of airspeed and altitude throughout the mission, that maximize range subject to thermal constraints on the components. Their work shows that trajectory shaping, in addition to airspeed selection, has potential to improve the performance of electric aircraft.

Justin et al. conducted a study of scheduled operations of electric commuter aircraft [14]. Recognizing the challenges associated with battery recharge time, they modeled operations with batteries that are interchangeable between flights, and posed and solved an optimization problem for recharging the swapped batteries to minimize the total cost of electricity for the airline operators.

The aforementioned examples of past research all indicate that electric aircraft should be sized and operated in new ways to realize their full potential. This work seeks to contribute new, optimal ways to operate electric aircraft for scheduled air transportation services by considering optimal flight speeds that balance the flight energy expenditure with ground recharge time.

III. Problem Formulation

In this section, we develop the schedule model, vehicle model, flight profile, and optimization problem formulation used throughout this work.

A route-schedule is defined as a sequence of n routes, each specified by four parameters: 1) the route's index i in the sequence; 2) the distance of the flight R_i; 3) the total time Δt_i allowed between departures of flight i and $i+1$, which includes the time available for flight i and any subsequent ground operations, including recharge; and 4) the recharging power available at the destination P_i.

A notional route-schedule parameterized in this way is illustrated in Fig. 1. The figure depicts the variation of battery state of charge vs time for three flights, each followed by a recharge. The variable $\Delta\chi_{f,i}$, which measures the energy expended in flight, is a function of R_i and the associated flight speed. The variable $\Delta\chi_{r,i}$, the energy recharged, is a function of P_i and the time available for recharge. The time between departures Δt_i defines the required route time interval and is indicated at the top of the figure.

The objective of this paper was to determine how to choose cruise airspeeds to maximize the energy feasibility of route-schedules for battery-electric aircraft. A route-schedule becomes energy infeasible if the vehicle must discharge its battery below a minimum capacity threshold during any flight in the schedule. The threshold includes an appropriate buffer to complete a reserve mission and to avoid the highly nonlinear drop in voltage associated with low states of charge. It is apparent that the point in the schedule that results in the lowest state of charge is the most constraining. This state of charge is therefore an appropriate measure of the energy feasibility of the schedule. Therefore, the objective of this paper is to maximize the minimum state of charge that occurs in the schedule. Unless specified otherwise, all optimal airspeeds in this work maximize the schedule minimum state of charge, which is equivalent to maximizing the energy feasibility of the schedule.

A flight profile must be defined to further formulate the problem and to state an objective function for the optimization problem. A simple profile is used to maintain transparency and focus on the overall schedule energy problem. The vehicle is assumed to fly route i at cruise altitude and airspeed from the moment of takeoff until landing, and is assumed to recharge from the moment of landing until takeoff for route $i+1$. Other segments, such as climb, descent, and ground operations, could be included in a simple fashion, as discussed in Sec. VIII.

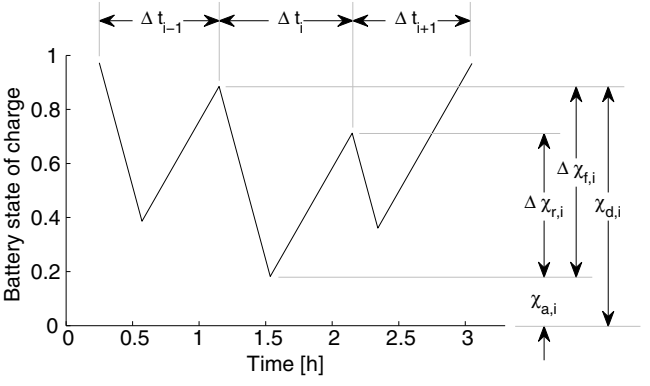

Fig. 1 Notional state of charge vs time for three routes.

The energy-feasibility objective requires accounting of the state of charge. Because battery discharge occurs only during flight, it is sufficient to account for the state of charge only at the end of every flight. The charge available at the arrival of a flight is the charge at departure less the flight discharge:

$$\chi_{a,i} = \chi_{d,i} - \Delta\chi_{f,i} \tag{2}$$

The flight discharge is calculated from Eq. (1) solved for the state of charge:

$$\Delta\chi_{f,i} = \left(\frac{D}{L}\right)_i \cdot W \cdot \frac{R_i}{\eta_p \cdot W_b \cdot \epsilon} \tag{3}$$

Note that $(L/D)_i$ is a function of airspeed for an aircraft, with a specified drag polar, in steady, level flight. The charge available at departure is the sum of the charge at arrival and the charge recouped during recharging on the ground:

$$\chi_{d,i} = \chi_{a,i-1} + \Delta\chi_{r,i-1} \tag{4}$$

Note that Eqs. (2) and (4) collectively define a recursion relation for arrival state of charge. The recharge energy is modeled simply as a product of recharge time and power normalized by the battery capacity:

$$\Delta\chi_{r,i} = \Delta t_{r,i} \cdot \frac{P_i}{W_b \cdot \epsilon} \tag{5}$$

The objective function can now be stated as

$$\max_{\{V_1,\ldots,V_n\}} (\min\{\chi_{a,1}, \ldots, \chi_{a,n}\}) \tag{6}$$

in which it is understood that the route index is an integer from 1 to n, and that $\chi_{a,0} \triangleq 1$ and $\Delta\chi_{r,0} \triangleq 0$.

A route-schedule implies constraints on energy because routes have a given range. The energy constraint for a given aircraft and mission requires that the energy needed to complete the mission be less than the energy available for the mission, with consideration of appropriate reserves. For the route-schedule, this is stated as

$$\chi_{a,i} \geq \chi_T \tag{7}$$

A period of ground operations may, in general, provide more than enough time to fully charge the battery. Any additional time, however, may not be used to overcharge the battery, because this would cause damage and may yield a false-positive feasibility for a schedule. A constraint is required to prevent this eventuality. Because recharge results only from ground operations, it is sufficient to apply this constraint only at the start of every flight:

$$\chi_{d,i} \leq 1 \tag{8}$$

Note that Eqs. (7) and (8) are recursive. The charge constraints for any route depend on the charge states of the previous route, and the previous route's constraints may or may not have been active. This complexity is a major source of the difficulty of the route-schedule energy problem.

A route-schedule implies constraints on time because the departure time for each flight is assumed fixed. If the aircraft is scheduled to depart at a particular time, it follows that there are limits to the airspeeds and recharge times of the preceding routes. The departure constraints can be expressed as

$$V_i \geq \frac{R_i}{\Delta t_i} \tag{9}$$

$$\Delta t_{r,i} \leq \Delta t_i - \frac{R_i}{V_i} \tag{10}$$

The optimization problem formulation used throughout this paper is now complete as defined by Eqs. (6–10).

IV. Route-Schedule Airspeeds

The best choice of airspeed for any given route in a schedule must balance the need to spend less energy flying that route to improve schedule-wide feasibility, the need to recharge the battery before the next route begins, and the need to arrive on time so that the subsequent route departure is not delayed. For example, if route i has the lowest arrival state of charge by a wide margin, then the choice of V_i should minimize the flight energy of route $i+1$, $\Delta\chi_{f,i}$, and the choice of V_{i-1} should maximize the battery charge at the start of route i, $\chi_{d,i}$. The choice of both V_i and V_{i-1} should respect Eq. (9). Solutions for the airspeeds that meet these criteria are necessary to solve the general airspeed selection problem and are derived as follows. The properties of these airspeeds are then explored and placed into the context of the general airspeed selection problem.

A. Derivation of the Airspeeds

The airspeed must be fast enough to maintain schedule timeline feasibility. The minimum airspeed required for this goal, which we term the "minimum schedule airspeed," is denoted $V_{S,i}$. Recall from Eq. (9) that this airspeed is

$$V_{S,i} = \frac{R_i}{\Delta t_i} \tag{11}$$

The route-schedule constraints depend on both the vehicle design and the airspeed. As implied by Eqs. (7–10), a relationship between airspeed and flight energy must be provided to understand the implications on route-schedule feasibility. To determine this relationship, presume a two-parameter quadratic drag polar model with parasite drag defined as

$$D_0 = C_{D0} \cdot 0.5 \cdot \rho \cdot V^2 \cdot S \tag{12}$$

and induced drag defined as

$$D_I = \frac{L^2}{\pi \cdot e \cdot b^2 \cdot 0.5 \cdot \rho \cdot V^2} \tag{13}$$

Substituting Eqs. (12) and (13) into Eq. (3), with the assumption of steady, level flight results in the desired relationship for change in state of charge in terms of airspeed

$$\Delta\chi_{f,i} = \left(C_{D0} \cdot S \cdot 0.5 \cdot \rho \cdot V_i^2 + \frac{W^2}{\pi \cdot e \cdot b^2 \cdot 0.5 \cdot \rho \cdot V_i^2}\right) \cdot \frac{R_i}{W_b \cdot \eta_p \cdot \epsilon} \tag{14}$$

The airspeed for the minimum energy per unit range, which we term the "Breguet speed," follows by differentiating Eq. (14) with respect to airspeed and setting the result equal to zero. The result is Eq. (15):

$$V_B = \sqrt[4]{\frac{W^2}{\pi \cdot e \cdot b^2 \cdot C_{D0} \cdot 0.25 \cdot \rho^2 \cdot S}} \tag{15}$$

which is the familiar airspeed for minimum drag in steady, level flight that causes the induced drag to equal the parasite drag, or

$$D_0 - D_I = 0 \tag{16}$$

Because Eq. (14) is convex, it follows that $V_i = V_B$ globally minimizes $\Delta\chi_{f,i}$.

The solid line in Fig. 2 depicts $\Delta\chi_f$, as computed from Eq. (14), for several values of airspeed, normalized by V_B, for a representative thin-haul electric aircraft flight. The parameter values used for all calculations throughout this paper are provided in Table 1.

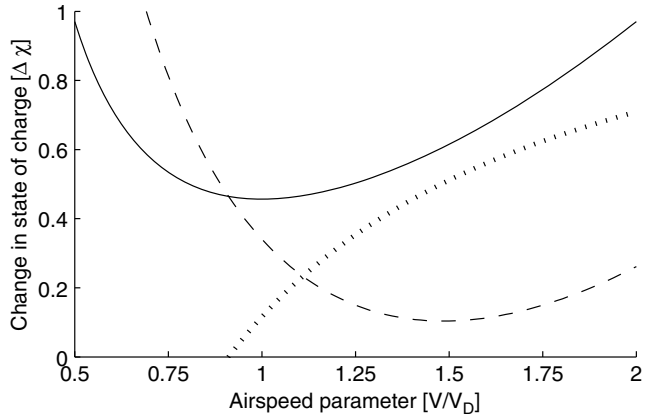

Fig. 2 Representative values of $\Delta\chi_f$ (solid), $\Delta\chi_r$ (dotted), and $\Delta\chi_n$ (dashed).

As expected, $\Delta\chi_f$ is minimized at $V/V_B = 1$. V_B is a key property of the vehicle design; it will be useful for simplifying performance relationships in later discussions. From V_B follows the minimum drag and the minimum battery output power required for steady, level flight:

$$D_B = C_{D0} \cdot S \cdot \rho \cdot V_B^2 = 4 \cdot \frac{W^2}{\pi \cdot e \cdot b^2 \cdot \rho \cdot V_B^2} \tag{17}$$

$$P_B = \frac{D_B \cdot V_B}{\eta_p} \tag{18}$$

A similar derivation provides the "maximum charge airspeed," $V_{\chi,i}$, for route i that maximizes the battery state of charge immediately preceding the departure of flight $i+1$. The initial charge of route i is $\chi_{d,i}$, and so setting $V_i = V_{\chi,i}$ results in the $\Delta\chi_{f,i}$ and $\Delta\chi_{r,i}$ that maximize $\chi_{d,i+1}$. Define the net discharge of route i as $\Delta\chi_{n,i} \triangleq \Delta\chi_{f,i} - \Delta\chi_{r,i}$. It follows from Eqs. (2) and (4) that $V_{\chi,i}$ minimizes $\Delta\chi_{n,i}$. Presume that $\Delta t_{r,i} = \Delta t_i - (R_i/V_i)$ to satisfy the equality in constraint Eq. (10), because the purpose of $V_{\chi,i}$ is to maximize the final state of charge. Using Eqs. (5) and (14), we can obtain an expression for $\Delta\chi_{n,i}$ and set $d\Delta\chi_{n,i}/dV_i = 0$. Through this process, and by simplifying with Eqs. (17) and (18), $V_{\chi,i}$ is obtained as the airspeed that satisfies Eq. (19):

$$\left(\frac{V_{\chi,i}}{V_B}\right)^4 - \frac{P_i}{P_B} \cdot \frac{V_{\chi,i}}{V_B} - 1 = 0 \tag{19}$$

The airspeed is given the subscript i, because it depends on the recharge power at the destination of route i.

The net discharge, $\Delta\chi_{n,i}$, determined by Eq. (14) minus Eq. (5) with $\Delta t_{r,i} = \Delta t_i - (R_i/V_i)$, is plotted as the dashed line in Fig. 2 for the parameters in Table 1 and a recharger with 500 kW power. The minimum occurs at $V_{\chi,i} \approx 1.5 \cdot V_B$ for this example. A more fundamental relationship, analogous to Eq. (16), can be established by rearranging Eq. (19) and expressing V_B and P_B in terms of D_0, D_I, and η_p to indicate the balance between parasite power, induced power, and recharge power required to minimize $\Delta\chi_{n,i}$:

$$2 \cdot \frac{D_0 \cdot V_{\chi,i}}{\eta_p} - 2 \cdot \frac{D_I \cdot V_{\chi,i}}{\eta_p} = P_i \tag{20}$$

Table 1 Notional example aircraft model, atmosphere, and constraint parameters

Symbol	Value	Units
W	8000	lb
W_b	1400	lb
S	250	ft^2
b	50	ft
e	0.75	
C_{D0}	0.025	
η_p	0.8	
W_b	3000	lb
ϵ	240	(W · h)/kg
	0.1459	(hp · h)/lb
χ_T	0.25	
ρ	0.001755	slug/ft^3

B. Properties of the Maximum Charge Airspeed

Several observations about $V_{\chi,i}$ are noteworthy. First, note that Eq. (19) has exactly one positive real root, and that the difference of Eqs. (5) and (14) is convex. These considerations imply that $V_{\chi,i}$ exists, is unique, and globally maximizes $\chi_{d,i+1}$. In other words, $V_{\chi,i}$ conserves the state of charge, from route to route, better than all other airspeeds.

Second, note that $V_{\chi,i} \to V_B$ as $P_i \to 0$, and the difference between $V_{\chi,i}$ and V_B for $P_i \neq 0$ is a result of the second term in Eq. (19). This term is strictly negative if the recharge power is positive. It follows that $V_{\chi,i} > V_B$, or, in other words, the airspeed that minimizes the net discharge is faster than the airspeed that minimizes drag.

This last finding is remarkable, because it may appear counterintuitive that using more energy could increase the feasibility of an energy-constrained schedule. Consider the situation, mentioned in Sec. I, in which ϵ, Δt_i, and P_i are sufficiently limited, such that the aircraft expends much more energy during each flight than it recovers by recharging. In this case, the lowest state of charge likely occurs during the final route, $i = n$, and so maximizing $\chi_{a,n}$ maximizes feasibility. It was just shown that $V_i = V_{\chi,i}$ should be chosen for all but the final route to maximize $\chi_{a,n}$ by maximizing $\chi_{d,n}$. Intuition may lead to choosing $V_i = V_B$ to maximize the feasibility of such an energy-constrained schedule because this minimizes energy usage. However, the additional energy expenditure to fly at $V_{\chi,i} > V_B$ is always more than offset by the additional recharge time recovered at the destination.

Third, note from Eq. (19) that $V_{\chi,i}$ increases as P_i increases. In other words, higher recharge power incentivizes higher flight speed. Taking the limit of Eq. (19) as $P_i \to \infty$ yields $V_{\chi,i} \to \infty$, which implies $\Delta\chi_{f,i} \to \infty$ for $V_i = V_{\chi,i}$. Hence, $V_{\chi,i}$ is irrelevant for a system with very high recharge power, because another objective will begin to dominate, or another constraint will become active, at a lower airspeed. This realization helps to illustrate an important difference between a vehicle with a rapid recharge capability, such as a fuel-burning or a battery-swapping aircraft, and a battery-recharging aircraft that may have limited recharge power. Fuel-burning or battery-swapping aircraft generally have no incentive to fly faster to increase schedule feasibility from an energetic perspective, because additional time on the ground does not enable greater range capability for subsequent flights.

C. Roles of the Airspeeds in the Optimization of Energy Feasibility

The three critical airspeeds—$V_{S,i}$, V_B, and $V_{\chi,i}$—define the interval of airspeeds for route i appropriate for achieving the schedule-wide maximum feasibility objective. Any airspeed $V_i \neq V_B$ results in suboptimal energy usage for route i, and $V_i < V_B$ also provides less charge available for route $i+1$. Any airspeed $V_i \neq V_{\chi,i}$ results in suboptimal charge available for route $i+1$, and $V_i > V_{\chi,i}$ also results in more energy usage. It is also clear from Eqs. (14) and (5) that the flight energy and charge available both change monotonically on the interval $[V_B, V_{\chi,i}]$ and that choosing V_i to improve one must degrade the other. It follows that, if $V_{S,i} < V_B$, then every route must be flown at an airspeed on the interval $[V_B, V_{\chi,i}]$ to maximize the minimum state of charge that occurs in the route-schedule. If the schedule is tight enough, then $V_{S,i} > V_B$, and the interval becomes $[V_S,\ V_{\chi,i}]$. If $V_{S,i} > V_{\chi,i}$, then $V_{S,i}$ is the optimum airspeed.

To help clarify its identity, the optimal airspeed interval formed from $V_{S,i}$, V_B, and $V_{\chi,i}$ will now be compared to classically known airspeeds that are optimal in different performance contexts. The airspeed for minimum power required is $3^{-0.25} \cdot V_B \approx 0.76 \cdot V_B$. This is slower than any airspeed in the optimal interval. The reason is that the objective is energy feasibility, which the problem formulation determines from route distance and not from a required flight time. Carson's speed is $3^{0.25} \cdot V_B \approx 1.32 \cdot V_B$, which is faster than V_B, but different from $V_{\chi,i}$. Carson's speed maximizes airspeed per unit energy spent [15], which is not equivalent to the energy-feasibility objective that determines $V_{\chi,i}$. Also notice that Carson's speed is a fixed multiple of V_B, but Eq. (19) implies that $V_{\chi,i}$ depends on P_i.

The interval formed from $V_{S,i}$, V_B, and $V_{\chi,i}$ must contain the optimal airspeed for the route. The interval boundaries are optimal for the routes in the example provided at the beginning of Sec. IV. It will soon also be apparent that, in general, the entire schedule must be specified to determine which particular airspeed in the interval is optimal.

Consider an example, in which the lowest state of charge in the schedule occurs on arrival of route i with $V_i = V_{\chi,i}$ and the vehicle does not fully recharge afterward. In this case, the state of charge on arrival of route i can be increased by flying slower. Doing so reduces the flight energy of route i, but also reduces the charge available for route $i+1$. Now, consider also that reducing the airspeed to $V_i = V_B$ causes route $i+1$ to have the lowest state of charge. Then, the optimal value of V_i, considering only routes i and $i+1$, must be the particular value between V_B and $V_{\chi,i}$ that provides the same lowest state of charge for both routes. This airspeed depends on the parameters of both routes. Therefore, it is necessary, in general, to fully define a schedule to fully determine the airspeed that is actually best for each route.

Two schedule optimization problems will be explored in the subsequent sections to determine the particular speeds between $V_{S,i}$, V_B, and $V_{\chi,i}$ that are optimal. In the first problem, every route is the same and repeating, and in the second problem, every route may have unique parameters.

V. Repeating Route-Schedules

Consider the problem of optimizing the cruise airspeed of a battery-electric aircraft for a schedule in which every route is identical. This type of schedule is referred to as a *repeating route-schedule*, and is representative of an aircraft that flies back and forth between a pair of destinations with a fixed time interval between each departure. Real flight schedules are not strictly repeating, but constant, averaged parameters can be chosen to obtain an approximately optimal repeating solution for many real-world schedules. Assume that the airspeed is restricted to be the same for all routes.

The repeating route-schedule simplifies the problem because Eqs. (3) and (5) imply that the discharge and recharge must be the same for every route. Furthermore, the vehicle either fully recharges before every departure and reaches the same state of charge at every arrival, or it never fully recharges and the battery discharges more deeply by the same amount on every route. Therefore, it is sufficient to apply Eq. (7) only to the last route in the schedule to ensure feasibility. Also, the recharge constraint Eq. (8) can now be handled with a single, schedule-wide condition, because a full recharge occurs for every route if it occurs for one route. The time constraints can also be handled with a single schedule-wide constraint. Finally, because all parameters are uniform, the sequence no longer matters and the subscript i is dropped for simplicity.

The optimal airspeed of a particularly constrained class of this schedule type is derived in the following subsection, along with other important, related quantities. These quantities will then be discussed for all other repeating route-schedules.

A. Charge-Draining Repeating Route-Schedules

Consider a class of schedules for which the battery either cannot be fully recharged, or can be fully recharged only if all available time is used and the airspeed is optimal. The airspeed that maximizes the charge available was shown to be V_χ in Sec. IV.A, but it will soon be clear that V_χ is not necessarily the optimal airspeed for this class of schedules. Let V'_χ be the new optimal airspeed. Furthermore, assume that $V'_\chi \geq V_S$, and so Eq. (9) is satisfied. In this case, there is never spare time on the ground left over after a recharge, and so $\Delta t_r = \Delta t - R/V$ and Eqs. (8) and (10) are satisfied. The state of charge vs time for an example schedule for this case is provided in Fig. 3. For this example, $R = 110$ n mile, $\Delta t = 1$ h, and $P = 500$ kW. Notice that the departure state of charge decreases for each subsequent route.

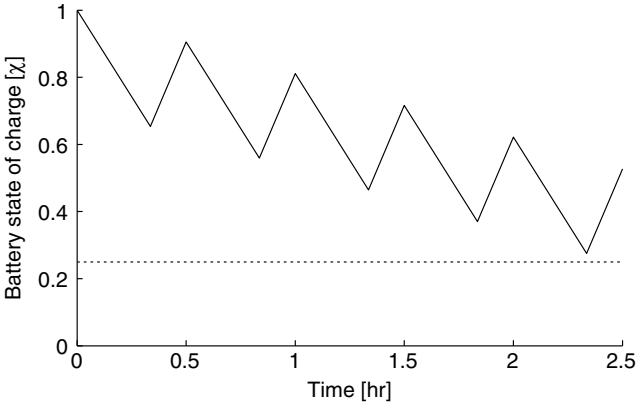

Fig. 3 Class 3 repeating route-schedule example; χ (solid) and χ_T (dotted).

The schedule minimum state of charge that occurs at the end of the final flight, $\chi_{a,n}$, can be calculated by summing the total flight energy of the n routes and subtracting the total recharged energy of the preceding $n-1$ routes. Using Eq. (14) for flight energy and Eq. (5) for recharge energy, and simplifying with Eqs. (15) and (17) result in Eq. (21), which satisfies Eq. (7):

$$\chi_T \leq \chi_{a,n} = 1 - n \cdot 0.5 \cdot \frac{R \cdot D_B}{W_b \cdot \eta_p \cdot \epsilon} \cdot \left(\left(\frac{V'_\chi}{V_B} \right)^2 + \left(\frac{V_B}{V'_\chi} \right)^2 \right) + (n-1) \cdot \frac{P \cdot \Delta t}{W_b \cdot \epsilon} \cdot \left(1 - \frac{V_S}{V'_\chi} \right) \tag{21}$$

These schedules are infeasible for all airspeeds if $\chi_{a,n} < \chi_T$ because V'_χ maximizes $\chi_{a,n}$. Set $d\chi_{a,n}/dV'_\chi = 0$ to find V'_χ. After rearranging, the result is a flight condition for this class of repeating route-schedules that is analogous to Eq. (20):

$$\frac{n}{n-1} \cdot \left(2 \cdot \frac{D_0 \cdot V'_\chi}{\eta_p} - 2 \cdot \frac{D_i \cdot V'_\chi}{\eta_p} \right) = P \tag{22}$$

Equation (22) represents a balance of parasite power, induced power, and recharge power very similar to the one that maximizes the charge available. By simplifying Eq. (22) with Eqs. (15), (17), and (18), V'_χ is obtained as the airspeed that satisfies Eq. (23):

$$\left(\frac{V'_\chi}{V_B} \right)^4 - \frac{n-1}{n} \cdot \frac{P}{P_B} \cdot \frac{V'_\chi}{V_B} - 1 = 0 \tag{23}$$

Note that Eq. (23) has exactly one positive real root and that Eq. (21) is convex. These considerations imply that V'_χ exists, is unique, and is globally optimal for this class of schedules.

Two facts about V'_χ are noteworthy. First, V'_χ is on the interval formed from V_S, V_B, and V_χ as required from Sec. IV.C. It can be shown through Eqs. (23) and (19) that $V_\chi > V'_\chi$. The difference of Eq. (22) and two times Eq. (18) implies that $V'_\chi > V_B$ if $P > 0$. Second, the location of V'_χ between V_S, V_B, and V_χ depends on n. The limit of Eq. (22) as $n \to \infty$ is Eq. (20), implying $V'_\chi \to V_\chi$. The limit of Eq. (22) as $n \to 1$ is Eq. (18), implying $V'_\chi \to V_B$.

These results support the conclusion that a fully defined schedule is generally necessary to find the optimum airspeed between V_S, V_B, and V_χ for any given route, as stated in Sec. IV.C. Also, intuition may lead one to anticipate that V_χ should be optimal because it minimizes

the net loss of charge for each route; however, the aforementioned relationships show that $V_\chi > V'_\chi$ for finite n. Choosing $V = V'_\chi$ provides a feasibility advantage over $V = V_\chi$ for small n, in which the discharge of a single route is more important. To see this, note that the objective of V'_χ is equivalent to minimizing $(n-1)\cdot\Delta\chi_n + \Delta\chi_f$, which is a weighted combination of the objectives that V_χ and V_B optimize.

The conditions under which V'_χ maximizes the schedule minimum state of charge can be expressed in terms of vehicle and schedule parameters. The necessary conditions stated earlier are equivalent to $\Delta\chi_r \le \Delta\chi_f$ and $V > V_S$. The vehicle would fully recharge with time left over if this condition were not satisfied. A slower speed could then enable a full recharge with less flight energy, yielding a higher minimum state of charge. Hence, $\Delta\chi_r \le \Delta\chi_f$ and $V > V_S$ are also sufficient to conclude that $V = V'_\chi$ is optimal. Using Eqs. (14) and (5) for $\Delta\chi_r$ and $\Delta\chi_f$; using Eq. (22) to eliminate V'_χ; and simplifying with Eqs. (11), (17), and (18) result in Eqs. (24) and (25), which are necessary and sufficient conditions under which V'_χ is the globally optimal airspeed:

$$\frac{P_B}{P} \ge \frac{2\cdot F\cdot(F-1)\cdot(V_B/V_S)^3}{F^4-(V_B/V_S)^4} \tag{24}$$

$$\frac{P_B}{P} \le \frac{n-1}{n}\cdot\frac{(V_B/V_S)^3}{1-(V_B/V_S)^4} \tag{25}$$

in which F is defined as

$$F \triangleq 0.5 + 0.25\cdot\frac{n-1}{n} + \sqrt{\left(0.5+0.25\cdot\frac{n-1}{n}\right)^2 + \frac{P_B}{P}\cdot\frac{V_B}{V_S}} \tag{26}$$

Note that these inequalities depend on an airspeed parameter, V_B/V_S; a power parameter, P_B/P; and n. Setting these parameters defines a repeating route-schedule for a given vehicle. The region for which V'_χ is optimal is plotted with vertical hatch lines in Fig. 4 for a continuum of schedules expressed in terms of V_B/V_S and P_B/P with $n = 8$.

B. Optimal Solutions for all Repeating Route-Schedules

There are three other classes of schedules plotted in Fig. 4 besides the one discussed previously. The class discussed previously will henceforth be denoted class 3. Proofs of class 3 optimal airspeed, its feasibility, conditions for global optimality, and resulting minimum state of charge were provided previously. Proofs of these parameters for classes 1, 2, and 4 discussed next are provided in the Appendix in a way analogous to the development for class 3 schedules discussed previously. The class descriptions and results are summarized as follows:

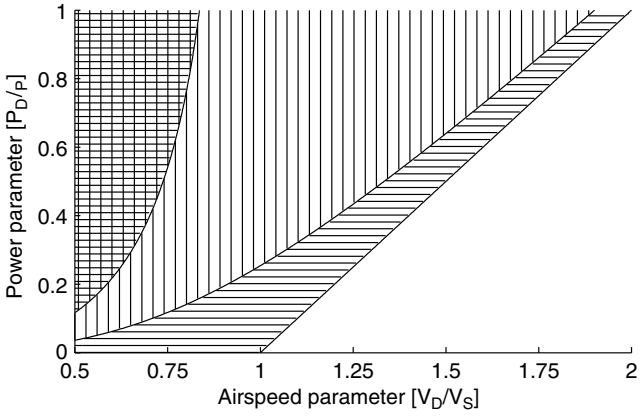

Fig. 4 Repeating route-schedule optimal airspeed regions with $n = 8$.

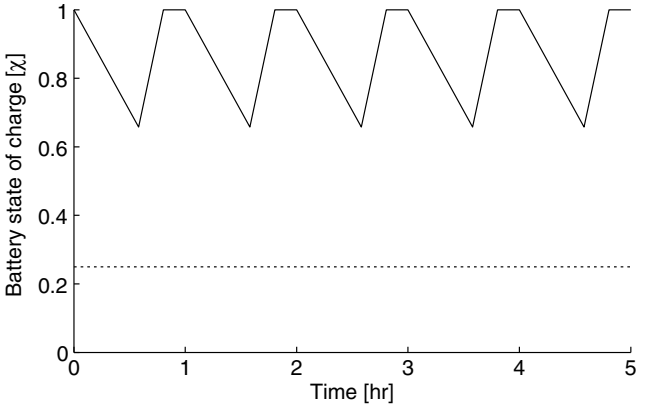

Fig. 5 Class 1 repeating route-schedule example; χ (solid) and χ_T (dotted).

1) Class 1: The aircraft can fully recharge even if it flies at the airspeed for minimum flight energy, V_B. Figure 5 shows an example state of charge vs time for this class of schedules. For this example, $R = 75$ n mile, $\Delta t = 1$ h, and $P = 500$ kW. Notice that some time is spent at a fully charged state ($\chi = 1$) before each departure. As proven in Appendix Sec. 2, the globally optimum airspeed is V_B, which is computed from Eq. (15).

Equation (27) is necessary and sufficient for the global optimality of V_B, and is plotted as white space in Fig. 4:

$$\frac{P_B}{P} \le \frac{V_B}{V_S} - 1 \tag{27}$$

The optimized energy constraint is Eq. (28):

$$\chi_T \le 1 - \frac{R\cdot D_B}{W_b\cdot\eta_p\cdot\epsilon} \tag{28}$$

2) Class 2: The aircraft can fully recharge if the vehicle is flown at some airspeed $V \ge V_B$. Figure 6 shows an example state of charge vs time for this class of schedules. For this example, $R = 100$ n mile, $\Delta t = 1$ h, and $P = 500$ kW. Notice that the aircraft departs for each subsequent route immediately after a full charge is obtained. As proven in Appendix Sec. 1, the globally optimum airspeed is V_E, which is the smallest positive real root of Eq. (29):

$$\left(\frac{V_E}{V_B}\right)^4 - 2\cdot\frac{P}{P_B}\cdot\frac{V_E}{V_S}\cdot\frac{V_E}{V_B} + 2\cdot\frac{P}{P_B}\cdot\frac{V_E}{V_B} + 1 = 0 \tag{29}$$

The intersection of Eqs. (30) and (31) is necessary and sufficient for the global optimality of V_E, and is plotted with horizontal hatch lines in Fig. 4:

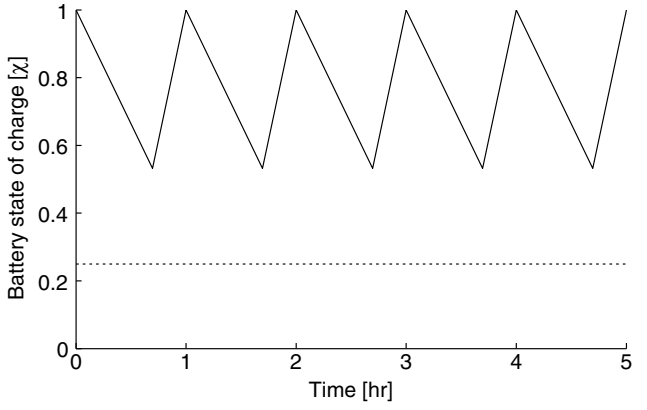

Fig. 6 Class 2 repeating route-schedule example; χ (solid) and χ_T (dotted).

$$\frac{P_B}{P} \geq \frac{V_B}{V_S} - 1 \tag{30}$$

$$\frac{P_B}{P} \leq \frac{2 \cdot F \cdot (F-1) \cdot (V_B/V_S)^3}{F^4 - (V_B/V_S)^4} \tag{31}$$

in which F is defined in Eq. (26). The optimized energy constraint is Eq. (32):

$$\chi_T \leq 1\text{–}0.5 \cdot \frac{R \cdot D_B}{\eta_p \cdot W_b \cdot \epsilon} \cdot \left(\left(\frac{V_E}{V_B}\right)^2 + \left(\frac{V_B}{V_E}\right)^2 \right) = 1 - \frac{P \cdot \Delta t}{W_b \cdot \epsilon} \cdot \left(1 - \frac{V_S}{V_E}\right) \tag{32}$$

3) Class 3: The airspeed is optimal and unconstrained, and the battery either cannot be fully recharged or can be fully recharged only if all available time is used. Figure 3 shows an example state of charge vs time for this class of schedules. Notice that the initial state of charge decreases route after route. As proven earlier in Sec. V.A, the globally optimum airspeed is V'_χ, which is the positive real root of Eq. (23). The intersection of Eqs. (24) and (25) is necessary and sufficient for the global optimality of V'_χ, and is plotted with vertical hatch lines in Fig. 4. The optimized energy constraint is Eq. (21).

4) Class 4: The unconstrained optimal airspeed is less than or equal to V_S. There is no time available for recharge, and so the state of charge decreases monotonically throughout the schedule. As proven in Appendix Sec. III, the globally optimum airspeed is V_S, which is computed from Eq. (11). Equation (33) is necessary and sufficient for the global optimality of V_S, and is plotted with crossed hatch lines in Fig. 4:

$$\frac{P_B}{P} \geq \frac{n-1}{n} \cdot \frac{(V_B/V_S)^3}{1 - (V_B/V_S)^4} \tag{33}$$

The optimized energy constraint is Eq. (34):

$$\chi_T \leq 1 - n \cdot 0.5 \cdot \frac{R \cdot D_B}{W_b \cdot \eta_p \cdot \epsilon} \cdot \left(\left(\frac{V_S}{V_B}\right)^2 + \left(\frac{V_B}{V_S}\right)^2 \right) \tag{34}$$

The four schedule classes discussed previously have dealt with every combination of active constraints. Therefore, the entire space of repeating route-schedules has been optimized, and the developments presented previously for each of the four repeating route-schedule-type regions in Fig. 4 represent the complete solution to the repeating route-schedule problem. The results are organized and presented in Table 2. Each row corresponds to one of the four classes of repeating route-schedules. The "airspeed value," "optimality conditions," and "energy constraint" columns reference the equations that determine the optimal airspeed value, conditions for global optimality, and resulting minimum state of charge, respectively. The optimality conditions define the boundaries of the regions in Fig. 4, which are called out in the "Fig. 4 plot region" column. The "proof" column indicates the section where the equations and properties of each class were proven.

VI. Nonrepeating Route-Schedule

The problem of optimizing the airspeeds of a battery-electric aircraft is now considered for a schedule, in which every flight may have a unique distance, time between departures, and destination recharge power. This type of schedule is referred to as a *nonrepeating route-schedule*. A nonrepeating route-schedule is more general and results in a more complex optimization problem than a repeating route-schedule. It is useful in the optimization of the operations of an existing aircraft that is to fly a particular sequence of routes. It is assumed that the airspeed may vary from route to route, as in the original optimization problem statement of Eq. (6), because R_i, Δt_i, and P_i may vary.

Recall from Sec. IV.C that the optimal airspeed for any route is on an interval defined by $V_{S,i}$, V_B, and $V_{\chi,i}$. The airspeed on this interval must be chosen separately for each flight in a nonrepeating route-schedule, whereas only a single optimal airspeed has to be chosen for all routes of a repeating route-schedule. The airspeeds, however, must be chosen in concert to maximize the lowest state of charge that occurs during the schedule.

To further complicate matters, it is not known a priori which routes cause the lowest state of charge or enable a full recharge. This information is deduced before optimization of the repeating route-schedule, because $\chi_{a,i}$ and $\chi_{d,i}$ are monotonic in i. For a nonrepeating schedule, however, the occurrence of full recharge or reaching the minimum state of charge cannot be determined without knowing the airspeeds, according to Eqs. (3) and (5). This is problematic, because the optimal airspeeds cannot be determined without this information. For example, if route i yields the lowest state of charge, it may be possible that increasing the airspeeds of routes 1 through $i-1$ would increase this state of charge.

Fortunately, the nonrepeating route-schedule airspeed optimization problem has two properties that can be exploited to enable an efficient algorithmic solution: greedy choice and optimal substructure. The difficulties described previously will be dealt with in the following discussions. A new optimal airspeed will be derived; a method for choosing between this new airspeed, $V_{S,i}$, V_B, and $V_{\chi,i}$ will be explained; and then the greedy choice and optimal substructure properties will be used to obtain an efficient implementation of the method.

A. Greedy Airspeed Policy

For the following discussions, consider route i of a given schedule with the goal of determining the globally optimal value of V_i for a given vehicle. Presume that the airspeeds for all other routes are already chosen and all attendant changes in state of charge are known. The following facts are useful in defining the airspeed optimization process.

1) Equations (2–5) imply that the states of charge for routes 1 through $i-1$ are not impacted by the choice of V_i. Therefore, V_i is chosen without regard for these routes, and the globally optimal value of V_i maximizes the lowest state of charge that occurs during routes i through n.

2) Defining $\chi_{\text{ms},i}$ as the lowest state of charge that occurs during routes $i+1$ through n, as in Eq. (35)

$$\chi_{ms,i} \triangleq \min\{\chi_{a,i+1}, \ldots, \chi_{a,n}\} \tag{35}$$

we can note that Eqs. (2–5) imply that $\chi_{ms,i}$ increases monotonically with $\chi_{d,i+1}$, the final state of charge of route i, and monotonicity holds even if a full recharge occurs during routes i through n.

3) As in the analysis of Sec. IV.C, Eqs. (2) and (14) imply that $\chi_{a,i}$, the lowest state of charge for route i, strictly decreases with increasing V_i on the interval $[V_B, V_{\chi,i}]$, and, when combined with Eqs. (4) and

Table 2 Solution to the repeating route-schedule problem

Class	Optimal airspeed	Airspeed value	Optimality conditions	Energy constraint	Fig. 4 plot region	Proof
1	V_B	Eq. (15)	Eq. (27)	Eq. (28)	White	Appendix Sec. 2
2	V_E	Eq. (29)	Eqs. (30) and (31)	Eq. (32)	Horizontal hatch lines	Appendix Sec. 1
3	V'_χ	Eq. (23)	Eqs. (24) and (25)	Eq. (21)	Vertical hatch lines	Sec. V.A
4	V_S	Eq. (11)	Eq. (33)	Eq. (34)	Crossed hatch lines	Appendix Sec. 3

(5), the equations imply that $\chi_{d,i+1}$ strictly increases with increasing V_i on the interval $[V_B, V_{\chi,i}]$.

From these facts, it is clear that the feasibility of the schedule, insofar as the choice of V_i can influence it, is limited by the lower of $\chi_{a,i}$ and $\chi_{\text{ms},i}$. It is also clear that improving either $\chi_{a,i}$ or $\chi_{\text{ms},i}$ will monotonically degrade the other. The optimal compromise is to choose V_i as high as possible on the interval $[V_B, V_{\chi,i}]$ without making $\chi_{a,i}$ lower than $\chi_{\text{ms},i}$, and setting $V_i = V_{S,i}$ if V_i would otherwise violate Eq. (9).

This airspeed policy has three outcomes, which depend on the value of $\chi_{\text{ms},i}$, for any given route:

a) The value is greater than $\chi_{a,i}$ even with $V_i = V_B$. The globally optimal airspeed is the faster of V_B and $V_{S,i}$, because all other values either strictly decrease $\chi_{a,i}$ or are infeasible.

b) The value is less than $\chi_{a,i}$ for all airspeeds. The globally optimal aispeed is the faster of $V_{\chi,i}$ and $V_{S,i}$, because all other values either strictly decrease $\chi_{\text{ms},i}$ or are infeasible.

c) The value is equal to $\chi_{a,i}$ for some airspeed, $V_i = V_{G,i}$, that satisfies $V_i > V_B$ and $V_i < V_{\chi,i}$. The faster of $V_{G,i}$ and $V_{S,i}$ is globally optimal, because all other values either strictly decrease $\chi_{a,i}$, strictly decrease $\chi_{\text{ms},i}$, or are infeasible.

A simple method of calculating the "greedy airspeed" $V_{G,i}$ is to set $\chi_{a,i} = \chi_{d,i} - \Delta\chi_{f,i} = \chi_{\text{ms},i}$ and substitute Eq. (14). By simplifying with Eqs. (17) and (18), $V_{G,i}$ is obtained as the airspeed that satisfies Eq. (36):

$$\left(\frac{V_{G,i}}{V_B}\right)^4 - 2 \cdot \frac{(\chi_{d,i} - \chi_{\text{ms},i}) \cdot W_b \cdot \epsilon \cdot \eta_p}{R_i \cdot D_B} \cdot \left(\frac{V_{G,i}}{V_B}\right)^2 + 1 = 0 \quad (36)$$

Note the following about $V_{G,i}$. First, Eq. (36) has no real solution if $\chi_{a,i} < \chi_{\text{ms},i}$ with $V_i = V_B$. Second, Eq. (36) has two real solutions if $V_{G,i}$ exists; one is less than V_B, and hence, $V_{G,i}$ is the larger one. Third, $V_{G,i} > V_{\chi,i}$ if $\chi_{a,i} > \chi_{\text{ms},i}$ with $V_i = V_{\chi,i}$, because $\chi_{a,i}$ monotonically decreases with increasing V_i. These facts are useful for an algorithmic implementation of the airspeed policy mentioned earlier. The optimal choice can now be made by determining whether $V_{G,i}$ exists, and comparing $V_{S,i}$, $V_{G,i}$, and $V_{\chi,i}$.

B. Greedy Algorithm for Choosing Optimal Airspeeds

It will now be shown that the nonrepeating route-schedule airspeed optimization problem has the greedy choice and optimal substructure properties. Suppose that $\chi_{\text{ms},i}$ is increased by setting the airspeeds of routes $i+1$ through n to newer, better values. It is clear, from the facts mentioned in Sec. VI.A, that a newer, better V_i may then increase the states of charge of only routes i through n. If V_{i+1} through V_n are globally optimal, then V_i can be globally optimized. The optimal solution of V_i therefore contains the optimal solution of V_{i+1} as a subproblem. It is also clear that the problem and subproblem have an identical structure. Therefore, it is evident that the nonrepeating route-schedule airspeed optimization problem has the optimal substructure property [16].

Suppose that optimal airspeeds are solved and assigned to routes in reverse order. Observe that the globally optimal choice for route i, as shown in the previous paragraph, is to maximize the minimum state of charge for routes i through n. This is also the local optimum from the perspective of route i, because optimization was completed without regard for routes 1 through $i-1$. Therefore, the nonrepeating route-schedule airspeed optimization problem also has the greedy choice property [16] if solved in reverse order. The optimization problem can therefore be solved efficiently with a greedy algorithm, because it has both the greedy choice and the optimal substructure properties [16]. The pseudocode of a suitable greedy algorithm is provided in Algorithm 1.

The assignment of recharge times has not been discussed, but must take place implicitly every time $V_{G,i}$ is evaluated for route i. This airspeed depends on the recharge times of routes $i+1$ through n by Eqs. (35), (7), and (8). The process of assigning recharge times is trivial; it is clear that they should be made as long as possible while still respecting Eq. (10). The optimal assignment of recharge times for routes $i+1$ through n can be reexecuted as the first step in the evaluation of $V_{G,i}$. Be careful of a new airspeed for route i changing $\chi_{\text{ms},i}$, because different routes may fully recharge.

Algorithm 1 Greedy algorithm for optimization of nonrepeating route-schedule airspeeds

```
χ_ms,i ← 1
for i = n to 1 do
  Evaluate V_G,i
  if V_G,i does not exist then
    V_i ← V_B
  else if V_G,i > V_χ,i then
    V_i ← V_χ,i
  else
    V_i ← V_G,i
  end if
  if V_i < V_S,i then
    V_i ← V_S,i
  end if
end for
```

VII. Example Results

Example results for repeating route and nonrepeating route-schedules are presented in this section. The results are reported for the example parameter values provided in Table 1.

A repeating route-schedule was simulated for three different airspeeds using the schedule parameter values $R = 100$ n mile, $\Delta t = 54$ min, and $P = 500$ kW. The resulting histories of battery state of charge vs time are provided, along with χ_T, in Fig. 7. This is a class 3 schedule according to Sec. V.B; the battery is depleted by a net discharge that builds up after each flight-and-recharge cycle, and the optimum airspeed is V'_χ.

The first state-of-charge history, indicated by the dashed line, corresponds to flight at a representative high-speed cruise with $V = 210$ KTAS. The second state-of-charge history, indicated by the solid line, corresponds to flight at the optimal airspeed, V'_χ, which is 179.1 KTAS in this case. Flying with $V = V_\chi$ enables two additional routes to be completed, relative to flying with $V = 210$ KTAS, before an additional route at the same V, R, and Δt becomes infeasible. The optimized schedule sacrifices some airspeed, while preserving departure times, to gain a substantial increase in feasibility. The third charge history, indicated by the dotted dashed line, corresponds to flight at the airspeed for minimum drag, V_B, which is 129.13 KTAS. The vehicle cannot complete the third route in this case because the low airspeed has reduced the recharge time.

A nonrepeating route-schedule was simulated for three different airspeed policies using the schedule parameters provided in Table 3. The resulting histories of battery state of charge vs time are provided,

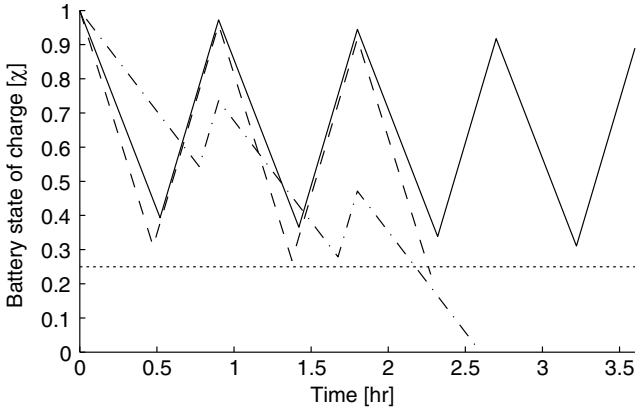

Fig. 7 State of charge resulting from several airspeeds in a repeating route-schedule.

Table 3 Nonrepeating route-schedule parameters and optimal airspeeds

i	R, n mile	Δt, min	P, kW	Airspeed type	Airspeed value, KTAS
1	27	15	500	$V_{\chi,1}$	192
2	79	30	500	$V_{\chi,2}$	192
3	79	33	500	$V_{\chi,3}$	192
4	79	48	500	$V_{G,4}$	131
5	53	22	500	$V_{G,5}$	169
6	22	25	500	V_B	129

along with χ_T, in Fig. 8. For this schedule, feasibility is quickly limited by the net discharge that accumulates after each flight-and-recharge cycle.

The optimal airspeed policy for a nonrepeating route-schedule is proven to be the greedy policy given in Sec. VI.A. The airspeeds chosen by this policy are recorded in the rightmost column of Table 3. The solid line in Fig. 8 is the state-of-charge history that results from these airspeeds. The optimum airspeeds for the first three routes are $V_{\chi,1}$, $V_{\chi,2}$, and $V_{\chi,3}$, which are 192 KTAS with $P_i = 500$ kW for all three. These were chosen because the accumulated discharge makes the later routes much more constraining. The optimal speeds for $i = 4$ and $i = 5$ are $V_{G,4}$ and $V_{G,5}$, respectively. Note that $\chi_{a,4} = \chi_{a,5} = \chi_{a,6}$ as expected. The final route is relatively short, but is the most constraining due to the accumulated discharge. Therefore, $V_6 = V_B$, which is 129 KTAS for this vehicle.

The dashed line in Fig. 8 is the state-of-charge history that results from an airspeed policy that chooses a representative high-speed cruise condition with $V_i = 210$ KTAS for every route. The dotted dashed line results from a policy that chooses $V_i = V_B = 129$ KTAS for every route. The optimal airspeed policy clearly provides a feasibility advantage over the other policies, enabling the completion of the last three routes.

VIII. Extension to More General Flight Profiles

The analyses presented throughout this paper are based on simple models of flight performance and route-schedules. The flight profile examined, which considers only cruise flight, is particularly simplistic: a typical transport mission consists of takeoff, climb, cruise, descend, and reserve segments, each requiring substantially different power levels. Furthermore, the energy spent in noncruise segments can be comparable to the energy spent in cruise for shorter flights.

Fortunately, the results detailed in this paper are readily extended to account for noncruise flight segments. This can be done by offsetting the range, time, and state of charge to account for all segments other than cruise, and then applying the analysis results to the optimization of the cruise airspeed only. In adopting this approach, however, it is required that the segment parameters not be coupled with the airspeed, and that the total range and time required by the noncruise segments not exceed that available in the schedule.

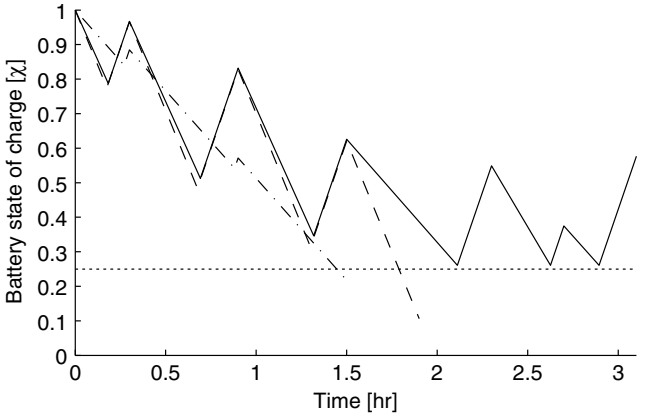

Fig. 8 State of charge resulting from several airspeeds in a nonrepeating route-schedule.

This approach to accounting other mission segments is as follows. Let $\Delta R_{s,i}$, $\Delta t_{s,i}$, and $\Delta \chi_{s,i}$ be the total distance, time, and charge consumed by all noncruise segments of route i, respectively. Equations (2) and (4–8) are unaffected by including noncruise segments. Affect the relevant changes by replacing R_i with $R_i - \Delta R_{s,i}$, Δt_i with $\Delta t_i - \Delta t_{s,i}$, and $\chi_{f,i}$ with $\chi_{f,i} - \Delta \chi_{s,i}$ in Eqs. (3), (9), and (10), and propagating these substitutions throughout all analyses. The substitutions have several noteworthy effects:

1) Equation (11) becomes $V_S = (R_i - \Delta R_{s,i})/(\Delta t_i - \Delta t_{s,i})$, which is interpreted as the minimum feasible airspeed for the cruise segment.

2) The term $\Delta \chi_{s,i}$ is eliminated during differentiation, and $\Delta R_{s,i}$ and $\Delta t_{s,i}$ cancel with V_S in Eqs. (15), (19), and (23). It follows that the values of V_B, V_χ, and V'_χ do not change, and still apply during cruise.

3) The new forms of V_S and ΔR_i alter Eqs. (29) and (36), respectively. The changes imply that V_E and $V_{G,i}$ apply during cruise, and take new values.

4) The new form of V_S changes the results of Eqs. (24), (25), (27), (30), (31), and (33).

5) The new form of V_S implies that the set of repeating route-schedules for which each airspeed is optimal depends on the cruise segment only.

6) Equations (14), (21), (28), (32), and (35) imply that $\Delta \chi_{s,i}$ and $\Delta t_{s,i}$ only decrease $\chi_{a,n}$ and $\chi_{\mathrm{ms},i}$, whereas $\Delta R_{s,i}$ only increases them.

What follows is an example application of the extension to a flight profile with only climb and cruise segments. Suppose that a climb segment is added before the cruise of the simplified flight profile in route i of a nonrepeating route-schedule, and that, after this is done, $V_{\chi,i}$ is the optimal airspeed for route i with $\chi_{d,i} = 1$, $R_i = 40$ n mile, $\Delta t_i = 20$ min, and $P_i = 500$ kW. The value of $V_{\chi,i}$ is the same regardless of the climb segment, but the value of $V_{G,i}$ may have changed. For illustration, we can evaluate $V_{G,i}$ according to Sec. VI to determine whether $V_{\chi,i}$ is optimal without the climb segment. Table 1 and Eqs. (15–18) provide $V_B = 129$ KTAS and $P_{B,i} = 193$ kW, which yield the optimum cruising speed, $V_{\chi,i} = 192$ KTAS, via Eq. (19). With no climb segment, the states of charge are $\chi_{a,i} = 0.479$ and $\chi_{d,i+1} = 1$ via Eqs. (2–10). Assuming the climb segment is executed at a maximum rate of climb speed of 115 KTAS and rate of climb of 1500 ft/min to 10,000 ft, the climb segment parameters are approximately $\Delta R_{s,i} = 12.7$ n mile, $\Delta t_{s,i} = 6.67$ min, and $\chi_{s,i} = 0.376$ in this case. Replacing R_i with $R_i - \Delta R_{s,i}$, Δt_i with $\Delta t_i - \Delta t_{s,i}$, and $\chi_{f,i}$ with $\chi_{f,i} - \Delta \chi_{s,i}$ in Eqs. (3), (9), and (10) provides the states of charge $\chi_{a,i} = 0.268$ and $\chi_{d,i+1} = 0.804$ via Eqs. (2–10).

IX. Conclusions

This paper has examined airspeeds for battery-electric aircraft that operate a scheduled service with a fixed departure timeline with recharges between flights. In particular, an optimization problem to maximize the energy feasibility of a route was posed and solved. The resulting optimal airspeeds maximize the schedule-wide minimum state of charge.

The optimization resulted in the identification of three airspeeds —$V_{S,i}$, V_B, and $V_{\chi,i}$—that form the interval that contains all possible airspeeds that maximize the schedule minimum state of charge. Particular airspeeds in this interval are optimal when a route-schedule is fully specified. These are V_S, V_B, V_E, and V'_χ for a repeating route-schedule, and these are $V_{S,i}$, V_B, $V_{G,i}$, and $V_{\chi,i}$ for a nonrepeating route-schedule.

A particularly interesting airspeed is V_χ. This speed represents a new important cruise operating point for battery-electric aircraft that must fly multiple routes sequentially and recharge on a time limit. It has a significance similar to the well-known minimum drag speed, V_B, that maximizes range for propeller aircraft. The derivation of V_χ clarifies important characteristics of the schedule problem. Some schedules become more feasible when an aircraft

flies certain routes at V_χ, a result that may be counterintuitive because V_χ is faster than V_B. Additionally, optimal airspeeds become faster with increasing recharge power and improved aerodynamics, and schedule feasibility increases with increasing recharge power and higher airspeeds.

The mission definition, drag polar, battery discharge, and range estimation models used in the mathematical developments in this paper are of the simplest forms, but they are general enough to illustrate the salient tradeoffs involved in airspeed optimization for electric aircraft in scheduled operations. This paper has shown how the mission definition is readily extended to include other segments. It would be straightforward to substitute improved models and to pursue the same general optimization strategy to refine the results. For example, it should be noted that the simple approach presented in Sec. VIII for handling noncruise mission segments would not be directly applicable to mission definitions, in which range credit for climb is allowed. In such a case, it would be desirable to select climb speed in addition to the cruise speed as part of the overall optimization problem.

This paper has focused on maximizing the energy feasibility for a schedule with a fixed departure timeline. Other meaningful objectives and operation models could be explored. For the sake of reducing electricity costs, it may be desirable to choose airspeeds to minimize the cumulative energy expenditure of a schedule. Another interesting formulation would allow the departure timeline to vary and would attempt to maximize the number of routes completed per unit time, which would be particularly relevant to on-demand air services. Such work will benefit from concepts that trade time and energy to increase both feasibility and flight speed.

Appendix: Proofs Related to Optimal Airspeeds

A.1. Class 2 Schedules and the Equal-Energy Airspeed

Consider a class of schedules for which the battery can be fully charged if the vehicle is flown at some airspeed $V \geq V_B$. Let V_E, the "equal-energy airspeed," be defined as the smallest airspeed for which flight energy is exactly equal to energy recharged with no spare recharge time. It is now shown that V_E is feasible. Equation (9) is satisfied because $V_E \geq V_S$ by definition. There is never spare time after recharge, and so Eq. (8) is always satisfied. It follows that $\Delta t_r = \Delta t - R/V$, which satisfies Eq. (10). The state of charge vs time of an example schedule for this case is provided in Fig. 6. Notice that the vehicle departs for each subsequent route immediately after a full charge is obtained.

It will now be shown that V_E is optimal if and only if the battery can be fully charged and $V_E \geq V_B$. First, note that, if Eq. (24) is not satisfied, then the vehicle can fully recharge with time to spare if $V = V'_\chi$. It follows that $V_E \leq V'_\chi$. Second, note that, if $V < V_E$, then a full recharge is not possible and the lower energy constraint is given by Eq. (21). Since $V_E \leq V'_\chi$ and V'_χ maximizes $\chi_{a,n}$ in Eq. (21), then $(d\chi_{a,n}/dV) \leq 0$ if V_E exists. It follows that no airspeed $V < V_E$ is optimal if V_E exists. Third, notice that, if $V_E \geq V_B$, then all airspeeds $V > V_E$ increase flight energy, but the additional recharge time provided by a higher airspeed does not help because the vehicle already fully recharges. It follows that no airspeed $V > V_E$ is optimal if $V_E \geq V_B$. Fourth, notice that, if $V_E < V_B$, then the vehicle can minimize the flight energy and also fully recharge the battery with time to spare with $V = V_B$. Therefore, V_E would not be optimal. Therefore, V_E is globally optimal if and only if $V_E \geq V_B$. It also follows that V_E is in the interval formed from V_S, V_B, and V_χ, as required in Sec. IV.C.

The conditions under which V_E maximizes the schedule minimum state of charge can now be expressed mathematically. V_E exists if and only if $\Delta\chi_r \geq \Delta\chi_f$ with $V = V'_\chi$, and is optimal if and only if $\Delta\chi_r \leq \Delta\chi_f$ with $V = V_B$. Combining Eqs. (14) and (5) with each inequality; using Eq. (22) to eliminate V'_χ; and simplifying with Eqs. (11), (17), and (18) result in Eqs. (30) and (31), which are necessary and sufficient conditions under which V_E is the globally optimal airspeed. Note that strict equality holds in Eq. (24) if and only if $V_E = V'_\chi$, which is true if and only if Eq. (31) is a strict equality. It follows that the set of schedules for which V_E is optimal is adjacent to the set for which V'_χ is optimal. The set for which V_E is optimal is plotted with horizontal hatch lines in Fig. 4 for a continuum of schedules expressed in terms of V_B/V_S and P_B/P, and for $n = 8$.

To obtain the energy constraint for this class of schedules, note that the lowest state of charge is the result of one flight or recharge: $\chi_a = 1 - \Delta\chi_f = 1 - \Delta\chi_r$. Substituting Eqs. (14) and (5) and simplifying with Eqs. (11) and (17) result in Eq. (32), which satisfies Eq. (7).

To compute V_E, rearrange Eq. (32) and simplify with Eq. (18) to obtain Eq. (29). If V_E exists, Eq. (29) has two positive real roots. The larger is greater than V'_χ, and hence, V_E is the smaller one.

A.2. Class 1 Schedules and the Breguet Airspeed

Consider a class of schedules for which the aircraft can fully recharge before every route even if it flies at the airspeed for minimum flight energy, V_B, which is determined by Eq. (15). It is now shown that V_B is feasible and optimal in this case. The battery fully recharges, and so $V_B \geq V_S$ and Eq. (9) is satisfied. There is always time for a full recharge; therefore, $\Delta t_r = (\Delta\chi_f \cdot W_b \cdot \epsilon)/P$ is optimal and satisfies both Eqs. (8) and (10). All airspeeds other than V_B increase flight energy, but cannot increase recharge energy. Therefore, V_B is optimal for these schedules according to Sec. IV.C. The state of charge vs time for an example from this class of schedules is provided in Fig. 5. Notice that some time is spent at a fully charged state ($\chi = 1$) before each departure.

The condition for this class of schedules is equivalent to $\Delta\chi_r \geq \Delta\chi_f$ with $V = V_B$. Combining Eqs. (5) and (14) with the inequality, and simplifying with Eqs. (11), (17), and (18) result in Eq. (27), which is a necessary and sufficient condition under which V_B is the globally optimal airspeed.

Note that strict equality holds in Eq. (30) if and only if $V_B = V_E$, which is true if and only if Eq. (27) is a strict equality. It follows that the set of schedules for which V_B is optimal is adjacent to the set for which V_E is optimal, and V_B is optimal if and only if $V_B \geq V_E$. The set for which V_B is optimal is plotted as a white space in Fig. 4 for a continuum of schedules expressed in terms of V_B/V_S and P_B/P, and for $n = 8$.

To obtain the energy constraint for this class of schedules, note that the battery always fully recharges. The lowest state of charge for repeating route-schedules that satisfy Eq. (27) is $\chi_a = 1 - \Delta\chi_f$ with $V = V_B$. Substituting Eq. (14) and simplifying with Eq. (17) result in Eq. (28), which satisfies Eq. (7).

A.3. Class 4 Schedules and the Minimum Schedule Airspeed

Consider the class of schedules for which V_S is the time-constrained optimum. Supposing Δt is varied while holding R, P, and the vehicle parameters fixed, V_S changes according to Eq. (11). If V_S is slow enough to permit a full recharge, Appendix Secs. 1 and 2 show that V_E exists, $V_E > V_S$, and the globally optimal airspeed would be V_B or V_E. However, if V_S is increased sufficiently, some of the time required for a full recharge becomes unavailable. Section V.A shows that V'_χ becomes globally optimal in this case. Now, note that V'_χ does not depend on V_S, according to Eq. (23). Increasing V_S further, so that $V_S \geq V'_\chi$, makes V'_χ either infeasible or equal to V_S, according to Sec. IV.C. Because Eq. (14) is convex and V_S becomes the slowest feasible airspeed, it follows that V_S is the constrained global optimum if and only if $V_S \geq V'_\chi$.

The condition, $V_S \geq V'_\chi$, is now shown in terms of vehicle and schedule parameters. Use Eq. (22) to eliminate V'_χ and simplify with Eqs. (11), (17), and (18). The result is Eq. (33), a necessary and sufficient condition under which V_S is the globally optimal airspeed.

Note that strict equality holds in Eq. (25) if and only if $V_S = V'_\chi$, which is true if and only if Eq. (33) is a strict equality. It follows that the set of schedules for which V_S is optimal is adjacent only to the set for which V'_χ is optimal. The set for which V_S is optimal is plotted with

crossed hatch lines in Fig. 4 for a continuum of schedules expressed in terms of V_B/V_S and P_B/P, and for $n = 8$.

To show that V_S is feasible, note that Eq. (11) satisfies Eq. (9) by identity. This implies that only $\Delta t_r = 0$ satisfies Eq. (10). Then, Eqs. (2–5) imply that Eq. (8) is always satisfied.

To obtain the energy constraint for this class of schedules, recall that there is no available recharge time. The final state of charge therefore results from n consecutive flights, and hence, $\chi_{a,n} = 1 - n \cdot \Delta\chi_f$. Substituting Eq. (14) and simplifying with Eqs. (15) and (17) result in Eq. (34), which satisfies Eq. (7).

Acknowledgments

This work was supported in part by NASA under grant NNX16AK24A, and via National Institute of Aerospace task order number 6565.

References

[1] Moore, M. D., and Fredericks, W. J., "Misconceptions of Electric Propulsion Aircraft and Their Emergent Aviation Markets," *52nd Aerospace Sciences Meeting, AIAA SciTech*, AIAA Paper 2014-0535, Jan. 2014.
doi:10.2514/6.2014-0535

[2] Stoll, A. M., and Mikić, G. V., "Design Studies of Thin-Haul Commuter Aircraft with Distributed Electric Propulsion," *16th AIAA Aviation Technology, Integration, and Operations Conference*, AIAA Paper 2016-3765, June 2016.
doi:10.2514/6.2016-3765

[3] Kreimeier, M., Gottschalk, D., and Stumpf, E., "Economical Assessment of Air Mobility on Demand Concepts with Focus on Germany," *16th AIAA Aviation Technology, Integration, and Operations Conference*, AIAA Paper 2016-3304, June 2016.
doi:10.2514/6.2016-3304

[4] Harish, A., Perron, C., Bavaro, D., Ahuja, J., Ozcan, M. D., Justin, C. Y., Briceno, S., German, B. J., and Mavris, D. N., "Economics of Advanced Thin-Haul Concepts and Operations," *16th AIAA Aviation Technology, Integration, and Operations Conference*, AIAA Paper 2016-3767, June 2016.
doi:10.2514/6.2016-3767

[5] Patterson, M. D., German, B. J., and Moore, M. D., "Performance Analysis and Design of On-Demand Electric Aircraft Concepts," *12th AIAA Aviation Technology, Integration, and Operations Conference*, AIAA Paper 2012-5474, Sept. 2012.
doi:10.2514/6.2012-5474

[6] Hepperle, M., "Electric Flight–Potential and Limitations," *NATO Workshop on Energy Efficient Technologies and Concepts of Operation*, NATO Science and Technology Organization STO-MP-AVT-209-09, Oct. 2012.
doi:10.14339/STO-MP-AVT-209

[7] Traub, L. W., "Range and Endurance Estimates for Battery-Powered Aircraft," *Journal of Aircraft*, Vol. 48, No. 2, March 2011, pp. 703–707.
doi:10.2514/1.C031027

[8] Doerffel, D., and Sharkh, S. A., "A Critical Review of Using the Peukert Equations for Determining the Remaining Capacity of Lead–Acid and Lithium–Ion Batteries," *Journal of Power Sources*, Vol. 155, No. 2, Dec. 2006, pp. 395–400.
doi:10.1016/j.jpowsour.2005.04.030

[9] Traub, L. W., "Validation of Endurance Estimates for Battery Powered UAVs," *Aeronautical Journal*, Vol. 117, No. 1197, Nov. 2013, pp. 1155–1166.
doi:10.1017/S0001924000008757

[10] Avanzini, G., and Giulietti, F., "Maximum Range for Battery-Powered Aircraft," *Journal of Aircraft*, Vol. 50, No. 1, Jan. 2013, pp. 304–307.
doi:10.2514/1.C031748

[11] Avanzini, G., de Angelis, E. L., and Giulietti, F., "Optimal Performance and Sizing of a Battery-Powered Aircraft," *Aerospace Science and Technology*, Vol. 59, Dec. 2016, pp. 132–144.
doi:10.1016/j.ast.2016.10.015

[12] Traub, L. W., "Optimal Battery Weight Fraction for Maximum Aircraft Range and Endurance," *Journal of Aircraft*, Vol. 53, No. 4, July 2016, pp. 1177–1179.
doi:10.2514/1.C033416

[13] Falck, R. D., Chin, J. C., Schnulo, S. L., Burt, J. M., and Gray, J. S., "Trajectory Optimization of Electric Aircraft Subject to Subsystem Thermal Constraints," *17th AIAA Aviation Technology, Integration, and Operations Conference*, AIAA Paper 2017-4002, June 2017.
doi:10.2514/6.2017-4002

[14] Justin, C. Y., Payan, A., Briceno, S., and Mavris, D. N., "Operational and Economic Feasibility of Electric Thin Haul Transportation," *17th AIAA Aviation Technology, Integration, and Operations Conference*, AIAA Paper 2017-3283, June 2017.
doi:10.2514/6.2017-3283

[15] Carson, B. H., "Fuel Efficiency of Small Aircraft," *Journal of Aircraft*, Vol. 19, No. 6, June 1982, pp. 473–479.
doi:10.2514/3.57417

[16] Cormen, T. H., Leiserson, C. E., Rivest, R. L., and Stein, C., "Greedy Algorithms," *Introduction to Algorithms*, 3rd ed., MIT Press, Cambridge, MA, 1990, pp. 414–443.
doi:10.2307/2583667